Pergamon

Carbon Vol. 35, No. 12, pp. 1689–1705, 1997

0008-6223/97 $17.00

PII: S0008-6223(97)00124-3

APPLICATION OF THE MONO/MULTILAYER AND ADSORPTION POTENTIAL THEORIES TO COAL METHANE ADSORPTION ISOTHERMS AT ELEVATED TEMPERATURE AND PRESSURE

C. R. CLARKSON,[a,*] R. M. BUSTIN[a] and J. H. LEVY[b]
[a]Department of Earth and Ocean Sciences, University of British Columbia, 6339 Stores Road, Vancouver, BC, Canada V6T 1Z4
[b]CSIRO Division of Coal and Energy, Menai, NSW, Australia

(*Received* 27 *November* 1996; *accepted in revised form* 12 *June* 1997)

Abstract—Accurate estimates of gas-in-place and prediction of gas production from coal reservoirs require reasonable estimates of gas contents. Equations based on pore volume filling/potential theory provide a better fit than the Langmuir equation to both high-pressure (up to 10 MPa), high-temperature ($>1.5T_c$) methane isotherm data, and low-pressure (<0.127 MPa) carbon dioxide isotherm data for 13 Australian coals. The assumption of an energetically homogeneous surface as proposed by Langmuir theory to the methane–coal system results in obtained with the assumption of liquid molar ures. Temperature-invariant characteristic curves are obtained for carbon dioxide, although further testing is required. The application of isotherms equations based upon pore volume filling/potential theory, in particular the Dubinin–Astakhov equation, have general validity in their application to high-pressure supercritical methane–coal systems as well as providing a better fit to isotherm data. © 1997 Elsevier Science Ltd

Key Words—A. Coal, C. adsorption.

1. INTRODUCTION

Recent interest in both recovery of natural gas from coal seams and in outburst hazards related to coal mining has led to extensive study of gas sorption in coal. The accurate prediction of coal gas capacities are important in gas reserve estimates and for input to production simulators. To simulate reservoir conditions, laboratory sorption isotherm data are generally collected at elevated temperature, usually between 0 and 50°C, and elevated pressure (up to 100 MPa). Methane gas sorption isotherms in coal, commonly Type I [1] in nature, are most often modeled using the Langmuir isotherm [2] and less frequently the Freundlich [3] or linear [4] isotherms. A study performed by Hall *et al.* compared the Langmuir model with various two-dimensional equations of state, the ideal adsorbed solution model, and loading ratio correlations for the adsorption of various gases and their mixtures on wet coal [5]. Only limited attention has been focused upon the application of adsorption potential theories to the description of methane adsorption isotherms collected for coals at elevated temperature and pressure [2]. Both the Dubinin–Radushkevich (D–R) and Dubinin–Astakhov (D–A) equations have been used to model Type I isotherms [1]. These isotherm equations are based upon the potential theory developed by Polanyi [6].

Ruppel *et al.* [2] applied the Langmuir and Polanyi adsorption models to methane adsorption isotherms collected for coals at temperatures ranging from 0 to 50°C and pressures from 10 to 150 atm (1–15 MPa). The Ruppel *et al.* study is the first detailing the application of adsorption-potential theory to methane sorption on dry coal at elevated temperature and pressure, although the model had previously been applied to other porous media under various conditions [7–10]. Ruppel *et al.* [2] found that the coal–methane adsorption system was well described by the Langmuir model, but the Polanyi theory did not accurately describe the system for all coals. It should be noted that thermal expansion of the adsorbate was not accounted for by Ruppel *et al.*, which, as shown in the case of activated carbons, may lead to the failure of one of the fundamental postulates of potential theory [11].

More recent studies [11,12] have applied Dubinin's volume filling theory, an adaptation of the original potential theory developed by Polanyi, to the high-pressure adsorption of various gases on activated carbon, in particular methane, above the critical point. These studies [11,12] outline the difficulties of applying the Dubinin postulates to supercritical fluids, such as the attainment of saturation vapour pressures and adsorbate densities. Agarwal and Schwartz [11] and Yang [13] provide a summary of the different approaches used to obtain these parameters. The desirability of using potential theory for the

*Corresponding author. E-mail: cclarkso@eos.ubc.ca

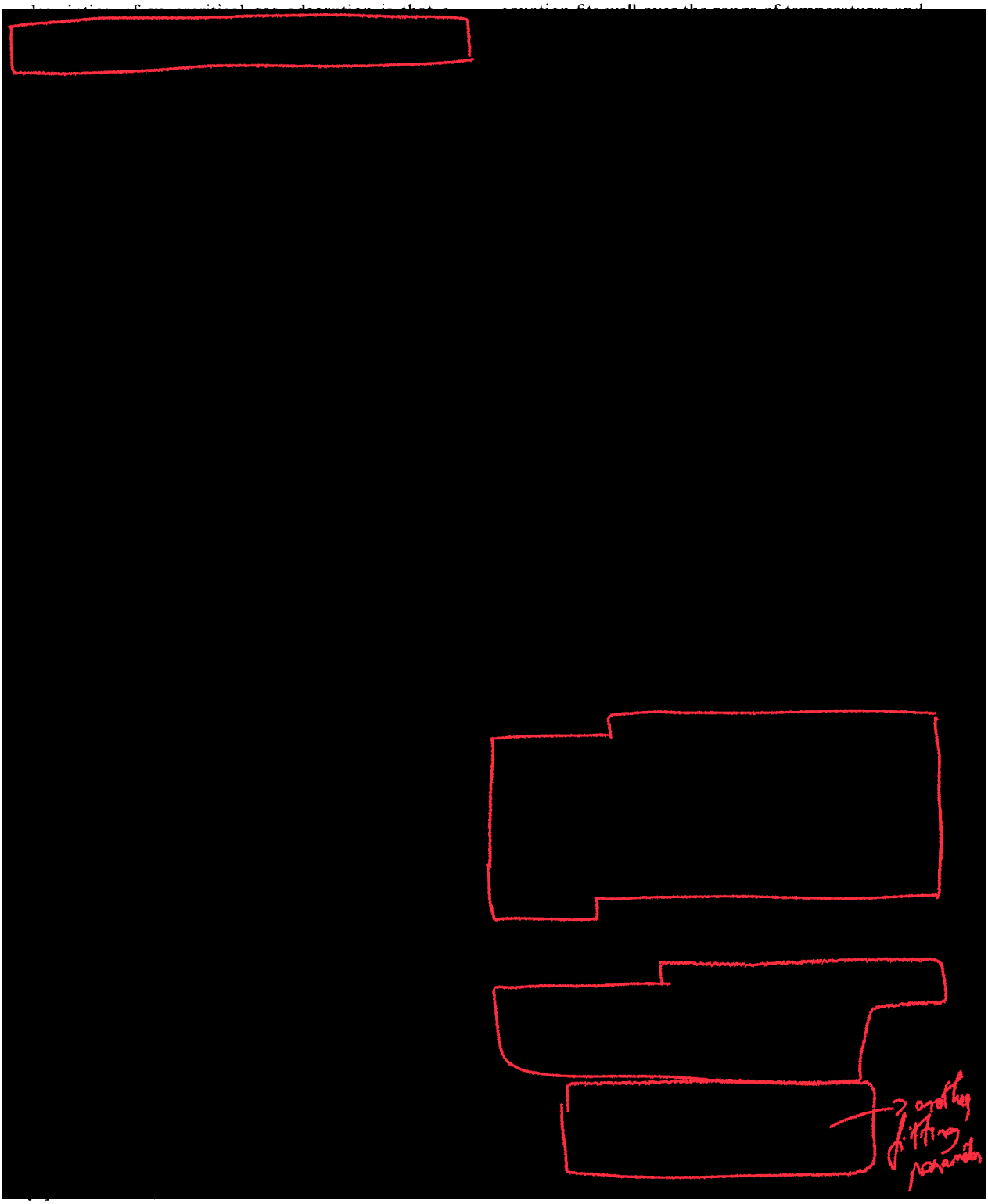

be energetically homogeneous with respect to adsorption. In many cases, a plot of P/V versus P yields a straight line whose slope yields V_m. The Langmuir model has frequently been applied to the description of Type I isotherms obtained for microporous solids such as activated carbons. Several studies of methane adsorption on coal have shown that the Langmuir

equilibrium, W_o is the micropore volume, β is a sorbate affinity coefficient, E is the characteristic energy, R is the universal gas constant, T is temperature, P_o is the saturation vapour pressure for the adsorbate, P is the equilibrium vapour pressure and n is a small integer (1–4) and is related to the distribution of pore sizes. These equations have been

applied to a variety of microporous solid–adsorbate systems. Recent work has focused upon the application of this theory to the adsorption of gases above

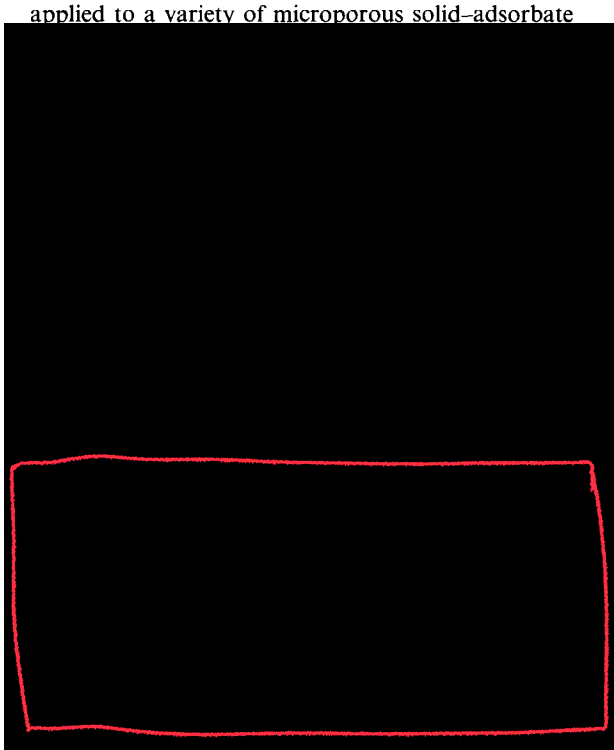

supercritical region for methane in various adsorption

desiccator was evacuated and placed in an oven set at 30°C; at least 48 hours were allowed for equilib-

Table 1. Maceral composition (vol%, mmf) and proximate analysis of samples studied

Sample	Telocollinite	Desmocollinite	Semifusinite	Fusinite	Inertodetrinite	Moisture (%)	Volatiles (%)	Fixed C (%)	Ash (%)
B1	9	24	34	33	–	0.9	20.3	68.6	10.2
B2	11	37	24	28	–	0.8	22.0	67.6	9.6
B3	10	39	37	14	–	0.7	21.8	68.9	8.6
B4	16	39	24	22	–	0.8	25.1	66.6	7.5
B5	30	36	20	15	–	0.7	25.4	64.1	9.8
B6	39	37	12	11	–	0.6	26.8	69.2	3.4
B7	90	0	1	9	–	0.7	21.8	67.7	9.8
W1	7	40	41	12	–	0.8	18.3	58.6	22.3
W2	13	54	18	15	–	0.6	24.6	59.4	15.4
W3	41	38	13	9	–	0.8	23.8	43.0	32.4
W4	62	31	4	3	–	1.0	21.7	58.0	19.3
W5	79	16	3	2	–	0.9	25.0	63.3	10.8
GHA1-09	13	48	24	1	14	1.4	24.1	67.0	7.5

rium prior to isotherm analysis. 10 or 11 pressure points were collected during isotherm analysis up to a pressure of about 10 MPa (absolute) for each sample. Equilibrium at each point is assumed to have been achieved if the pressure reading is constant ($\Delta P = 0.000$ MPa) over a 40 minute interval. Volumes of gas adsorbed are calculated using the Real Gas Law, and the void volume of the system, determined through helium expansion, is corrected for gas adsorbed at each pressure step, assuming liquid density of the adsorbate. Precision of isotherm runs is about $\pm 1\%$ relative.

Low-pressure (<0.127 MPa) carbon dioxide isotherms at 0°C were performed on dry (evacuated) coal samples on a Micromeritics ASAP 2010® automated volumetric gas sorption apparatus. In addition, the GHA1-09 sample was run at 25°C. Coal samples were evacuated at 100°C overnight to a pressure of <0.25 Pa prior to analysis. No non-ideality correction was made for carbon dioxide at these low pressures. A saturation vapour pressure of 3.48 MPa was used for carbon dioxide at 273 K and 6.42 MPa at 298 K. Precision of isotherm runs for coal is about $\pm 1\%$ relative. The instrument is periodi-

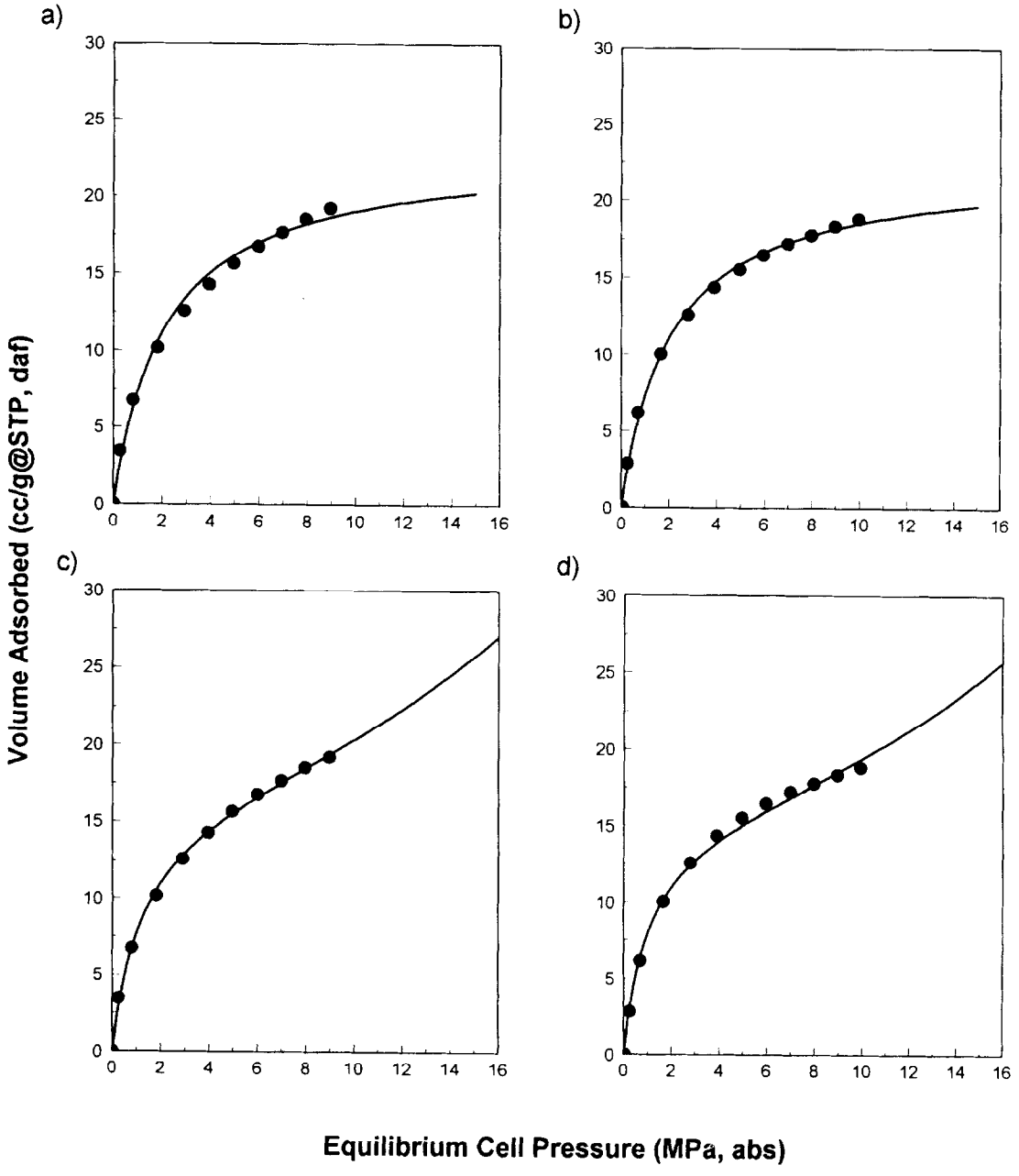

Fig. 1. Langmuir (a,b) and BET (c,d) curve fits to methane isotherm data for samples W1 (a,c) and B4 (b,d). Solid line is curve fit.

cally calibrated against a zeolite standard to check for systematic error.

2.3 *Langmuir, BET, D–R and D–A regression analysis*

The Langmuir isotherm was fit to the methane and carbon dioxide experimental data through the following procedure:

(1) A linear regression was performed for P/V versus P plots (referred to as Langmuir plots) and the Langmuir constants (B and V_m) were calculated from the slope and intercept.

(2) The calculated Langmuir sorbed volumes were obtained from the Langmuir equation in the usual form: $V=(V_mBP)/(1+BP)$.

(3) The Langmuir isotherm, plotted for 0.1 MPa pressure increments, was superimposed upon the experimental data.

(4) A similar procedure was followed for the BET analysis except a linear regression was performed upon $1/V(P_o/P-1)$ versus relative pressure plots (BET plots).

The saturation vapour pressure (or pseudo-saturation pressure) for the high-pressure/temperature methane analysis was obtained from the extrapolation of the log of vapour pressure, obtained from the CRC handbook [30], versus reciprocal of absolute temperature to the temperature of actual analysis. A similar procedure was used by Grant *et al.* [9]. This approach is compared against other methods in a later section. The values obtained from this extrapolation method agree most closely with values obtained from the use of the reduced Kirchoff equation as utilized by Kapoor *et al.* [23].

Dubinin regression analysis was performed in the following fashion:

(1) log V is plotted against $(\log P_o/P)^n$ (D–R or D–A transformed plots) and a least squares fit performed. For the D–R equation the value of n is equal to 2, but for the D–A equation the value of n is optimized by recalculating the linear regression until the standard error of the Y-intercept is minimized. The value of n is optimized to within 10^{-4}.

(2) The micropore capacity (V_o) is obtained from the Y-intercept.

(3) The calculated volumes adsorbed are obtained from eqn (4). The Dubinin isotherms are then plotted for 0.1 MPa increments and superimposed upon the experimental data.

Although conventional linearized unweighted regression models [2,15,31,32] were used to obtain fit parameters for the four isotherm equations, more refined and statistically rigorous regression models were also considered. Non-linear and non-linear weighted ordinary least squares (OLS) V on P, and non-linear weighted OLS P on V regression models were also applied to representative samples. These regression models more rigorously accommodate the proportional measurement error observed in pressure and volume adsorbed measurements. They have unbiased V residuals (see below), as opposed to the linearized regression model, which biases the V residual plots during transformation. Furthermore, comparison of the V on P and P on V non-linear weighted regression results allows determination of whether a regression model accommodating errors in both P and V variables is required.

Results from the different regressions were insig-

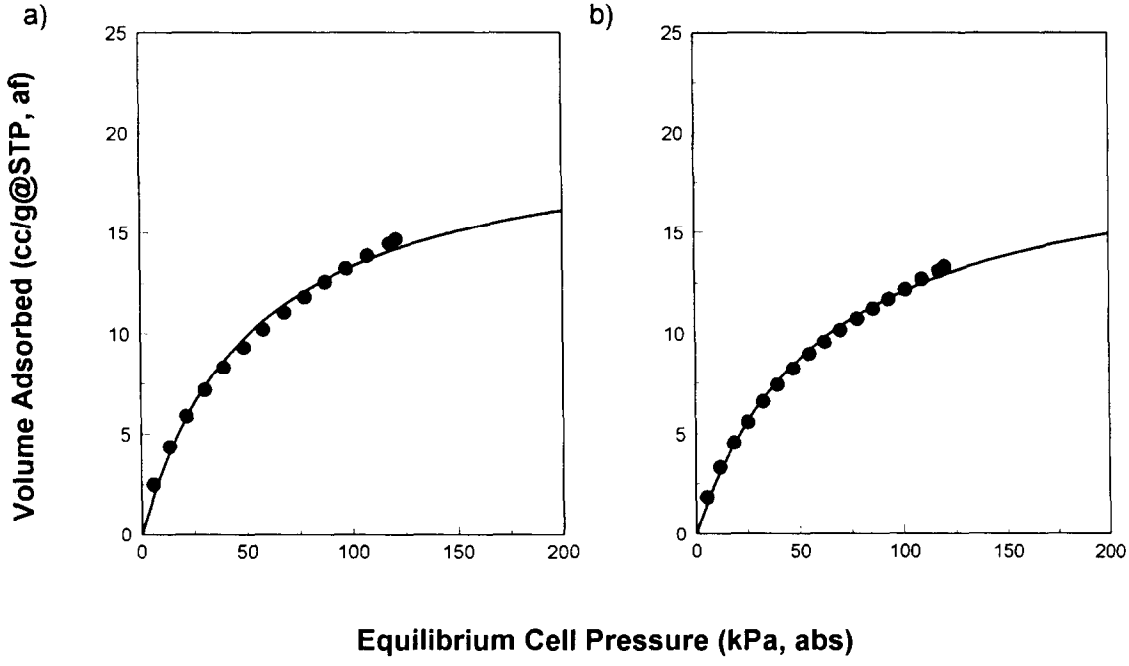

Fig. 2. Langmuir curve fits to carbon dioxide isotherm data for samples W1 (a) and B4 (b). Solid line is curve fit.

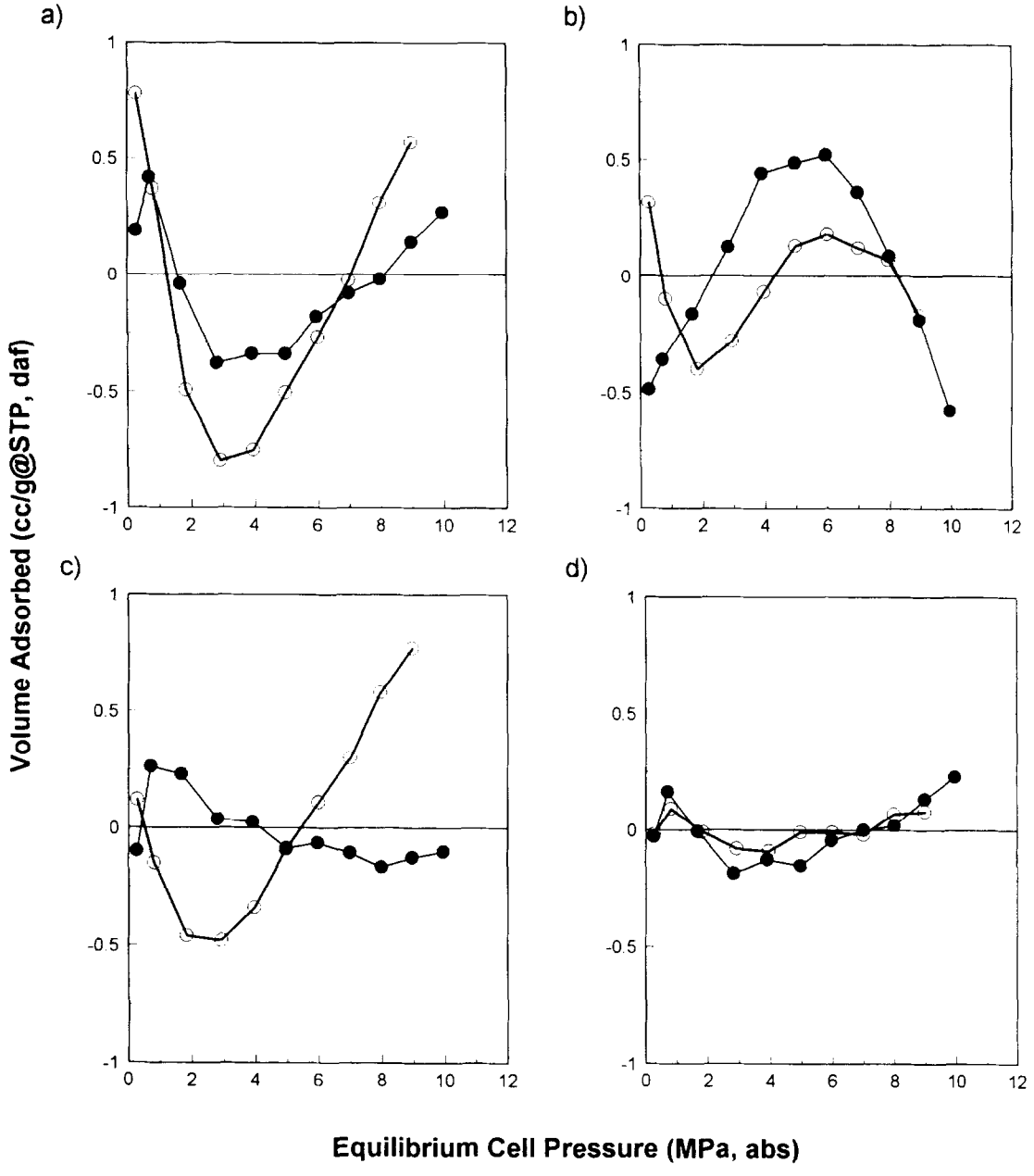

Fig. 3. Plots of residuals for Langmuir (a), BET (b), D–R (c) and D–A (d) curve fits. Samples are W1 (open circles) and B4 (solid circles).

nificantly different. This is a consequence of the relatively high degree of fit of all isotherm regression models. The average relative error (see below) averaged over all samples is less than 4.2, 2.1, 1.6 and 0.4% for the Langmuir, BET, D–R and D–A equations, respectively, regardless of the regression model applied. Results did not reorder the relative quality of fit for the four isotherm models (discussed below) and demonstrate that an "error in both variables" regression model is not required. Thus, although the non-linear weighted V–P regression model is the most consistent with the nature of the data and their errors, the conventionally applied linearized regression results are presented below in order to allow comparison with previous isotherm results (e.g. refs. [2,15]).

3. RESULTS

3.1 *Petrographic and proximate analysis*

The results of petrographic (maceral) and proximate analysis are presented in Table 1. Fixed carbon content of the Bulli seam samples ranges from 71 to 77% (dry, ash-free basis) whereas the Wongawilli seam values range from 64 to 76% [27]. Samples are composed mainly of the vitrinite macerals telocollin-

ite and desmocollinite, and inertinite macerals fusinite and semifusinite as well as mineral matter. Liptinite is rare.

3.2 *Langmuir correlations*

Correlation coefficients (r^2) calculated from linear regression analysis of the Langmuir plots (P/V vs P) are greater than 99% for all coals, and range from 99.06% (W1) to 99.85% (B4).

The calculated Langmuir isotherms (solid line) for the coals with the worst (W1) and best (B4) Langmuir correlations are shown in Fig. 1 along with the experimental high-pressure methane isotherms. The adsorbed volumes are presented on a dry, ash-free basis (DAF) and are corrected to standard temperature and pressure. The Langmuir isotherm calculated for W1 and B4 underestimates the volumes adsorbed at low (<2 MPa) and high pressure (>7 MPa) and overestimates the volume adsorbed in the mid-region of the isotherm (2–7 MPa). Although data for only two samples is shown here, the Langmuir isotherm breaks down in the same pressure region for all samples analyzed.

Langmuir isotherms are plotted for the low-pressure carbon dioxide analyses at 273 K (Fig. 2). The Langmuir plot r^2 values (not shown) are around

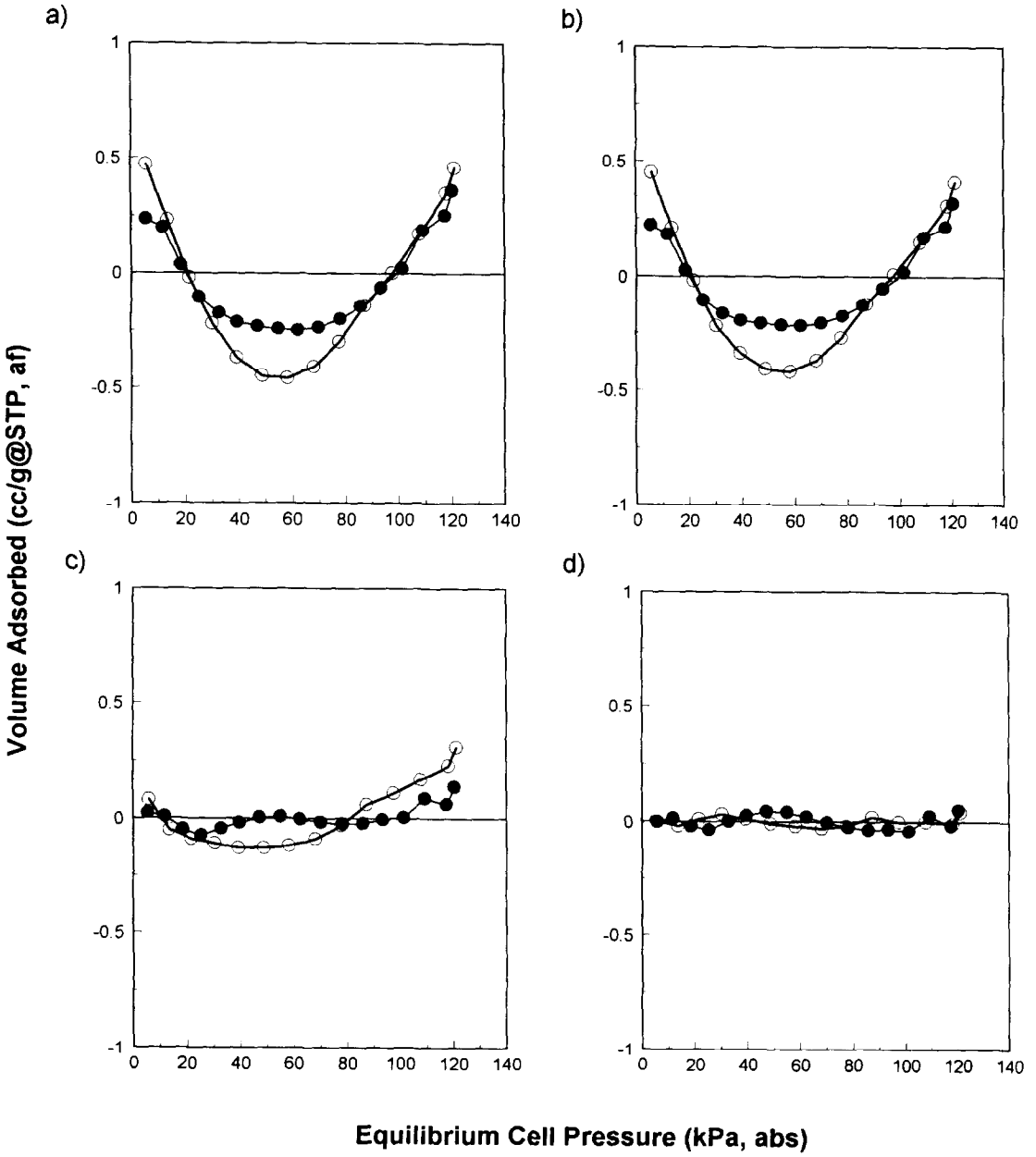

Fig. 4. Plots of residuals for Langmuir (a), BET (b), D–R (c) and D–A (d) curve fits. Samples are W1 (open circles) and B4 (solid circles). Carbon dioxide is the adsorbate used.

Table 2. Relative error calculations for isotherm fits

Average relative error					V_o (monolayer vol./micropore cap.)			
Sample	Langmuir (%)	BET (%)	D–R (%)	D–A (%)	Langmuir ($cm^{-3}g^{-1}$, DAF)	BET ($cm^{-3}g^{-1}$, DAF)	D–R ($cm^{-3}g^{-1}$, DAF)	D–A ($cm^{-3}g^{-1}$, DAF)
B1	3.05	1.82	0.67	0.67	21.4	15.1	20.8	20.7
B2	3.99	1.65	1.01	0.15	21.7	15.5	21.1	22.2
B3	3.93	2.65	1.14	0.36	21.7	15.0	20.9	21.9
B4	2.32	3.83	1.29	0.86	22.3	15.3	21.9	20.8
B5	4.18	1.48	1.06	0.47	22.3	15.9	21.7	22.6
B6	4.01	2.57	1.10	0.25	22.7	15.8	22.0	23.1
B7	4.29	1.63	1.18	0.62	21.4	15.2	20.7	21.9
W1	5.44	2.12	2.65	0.41	23.1	16.2	21.6	25.0
W2	4.86	1.95	2.49	0.37	24.8	17.3	23.1	26.3
W3	5.02	2.21	2.71	0.25	22.1	15.4	20.5	23.9
W4	5.31	1.78	2.31	0.77	23.9	16.8	22.5	25.4
W5	4.82	1.94	2.28	0.30	24.7	17.3	23.2	26.2
GHA1-09	2.71	2.19	0.86	0.31	23.2	15.6	21.7	22.6
Average (%)	4.15	2.14	1.60	0.45				

Average relative error (%) $= (100/N)\mathrm{Sum}(\mathrm{abs}(V_{cal} - V_{exp})/V_{exp})$.

99%, and the correlation for B4 (99.17%) is better than for W1 (98.50%).

A plot of the residuals, the difference between experimentally-determined and calculated adsorbed volumes of methane for the Langmuir fit, is shown in Fig. 3 for samples B4 and W1. The same trend is apparent for the low-pressure carbon dioxide analyses (Fig. 4), despite the difference in experimental conditions. It is important to note, however, that these plots may not be compared directly with the methane results as the isotherms for methane and carbon dioxide were run over much different relative pressure ranges (~0.001–0.3 for methane, and 0.002–0.035 for carbon dioxide).

In order to quantify the curve-fit for all samples, the average relative errors (*RE*) between the calculated and experimental adsorbed volumes of methane were determined (Table 2). The mean average relative errors for all samples tested is about 4.2% for the Langmuir correlation.

3.3 *BET correlations*

BET isotherms for samples W1 and B4 are shown in Fig. 1. BET plot (not shown) r^2 values are greater than 99% (99.71–99.92%), and are on average greater than the Langmuir values. The BET isotherm better fits the experimental data for sample W1 than the Langmuir isotherm (2.1% *RE* versus 5.0%), but not for B4 (3.8 versus 2.3%). In general, however, the BET isotherm provides a better fit to the high-pressure methane experimental data (Table 2).

A plot of the BET residuals for samples W1 and B4 is shown in Fig. 3. The opposite trend is observed than for the Langmuir residuals: the BET isotherm underestimates the volumes adsorbed in the middle region of the isotherm and overestimates at the low and high-pressure ends. This trend is obeyed for all samples studied. The same plot for carbon dioxide analyses (Fig. 4) illustrates that the BET residual trend is very similar to the Langmuir trend.

3.4 *D–R correlations*

D–R plots for the Australian coals are linear (not shown) and correlations are greater than 99% (99.66–99.98%) for all samples. The mean average relative error for the D–R fit for all samples is slightly lower than the BET fit (1.6 versus 2.1%). The D–R isotherm fit (Fig. 5) is better for sample B4 than for W1 and the residual plot trends (Fig. 3) are similar to that for the Langmuir fit. Residual plots are also shown for the carbon dioxide analyses (Fig. 4).

3.5 *D–A correlations*

The D–A equation yielded the highest correlations for the experimental data (99.96–100%); the mean average relative error for all samples is around 0.5%.

Table 3. Summary of the various methods used for the attainment of pseudo-saturation pressure and molar volume of the adsorbate

Pseudo-saturation pressure	Molar volume of adsorbate
$P_s = (T/T_c)^2$ [20]	$V = V_s(T_b)^a$
From reduced Kirchoff [22]	$V = V_s(T_b)\exp(\Omega(T - T_b))^b$ [10,21,25]
Extrapolated log *vp* versus $1/T$ plot[c]	

[a] $V_s(T_b)$ = liquid molar volume of the adsorbate at normal boiling point.
[b] Ω = thermal expansion coefficient of the adsorbate, taken as 0.0016 [10].
[c] *vp* = vapour pressure.

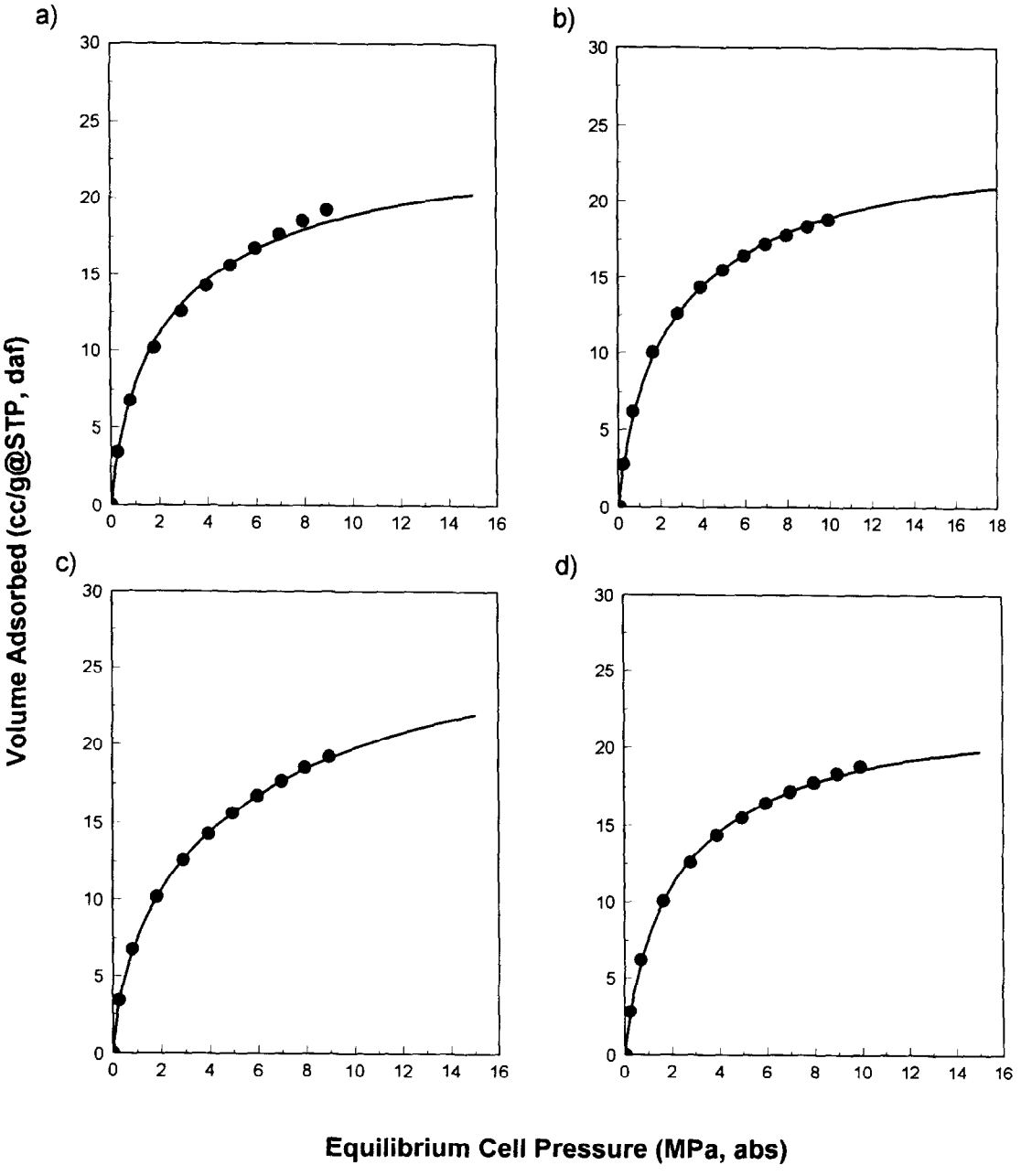

Fig. 5. D–R (a,b) and D–A (c,d) curve fits to methane isotherm data for samples W1 (a,c) and B4 (b,d). Solid line is curve fit.

Residual plots for samples W1 and B4 show no distinct trend (Fig. 3), which indicates an excellent fit to the data.

4. DISCUSSION

In general, for the coals studied, the isotherm equations based upon adsorption potential theory (D–R and D–A) yield a better curve-fit to the experimental data than those based upon the mono/multi-layer pore filling models (Langmuir and BET). Three equations are two-parameter models (Langmuir, BET and D–R) while the fourth is a three-parameter model (D–A). Both the BET and D–R equations yield better fits to the data than the Langmuir equation for all coals, except sample B4. Although all the isotherm equations applied yield a reasonable approximation to the experimental data, the validity of the underlying theories requires testing.

4.1 *Langmuir theory*

Criteria for Langmuir-type adsorption may be summarized as follows:

(1) The adsorption surface is energetically homogeneous.

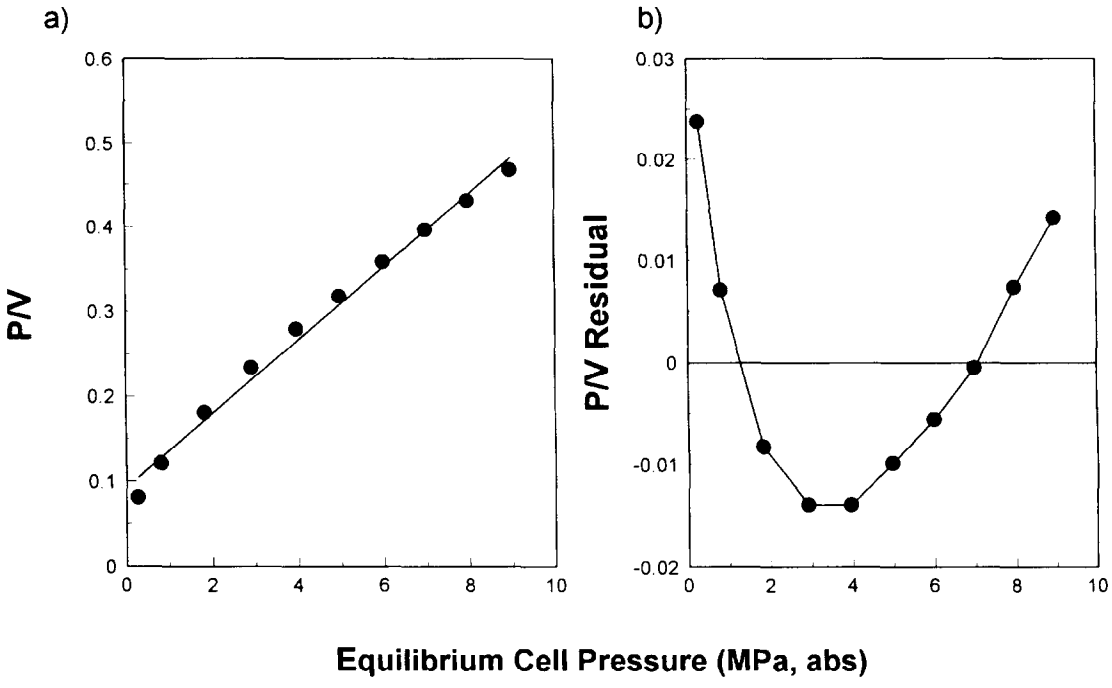

Fig. 6. Langmuir plot (a) and plot of residuals (b) for W1.

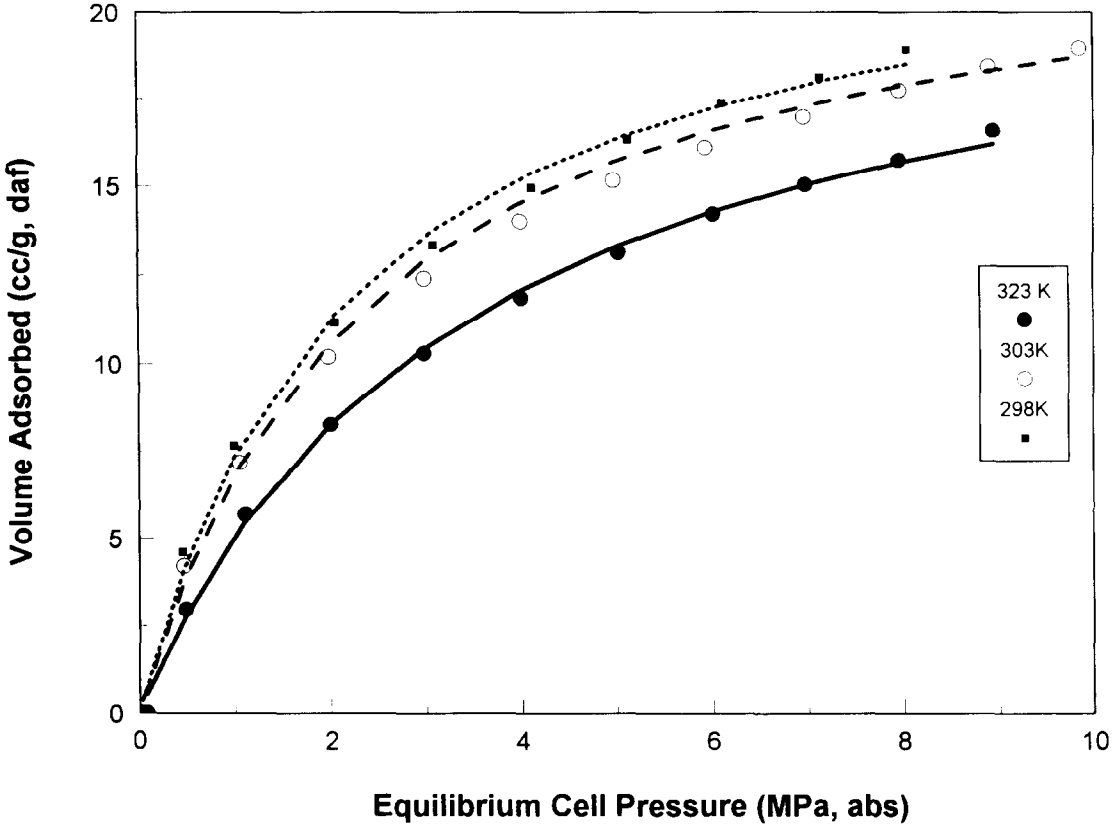

Fig. 7. Recalculated Langmuir isotherms for GHA1-09.

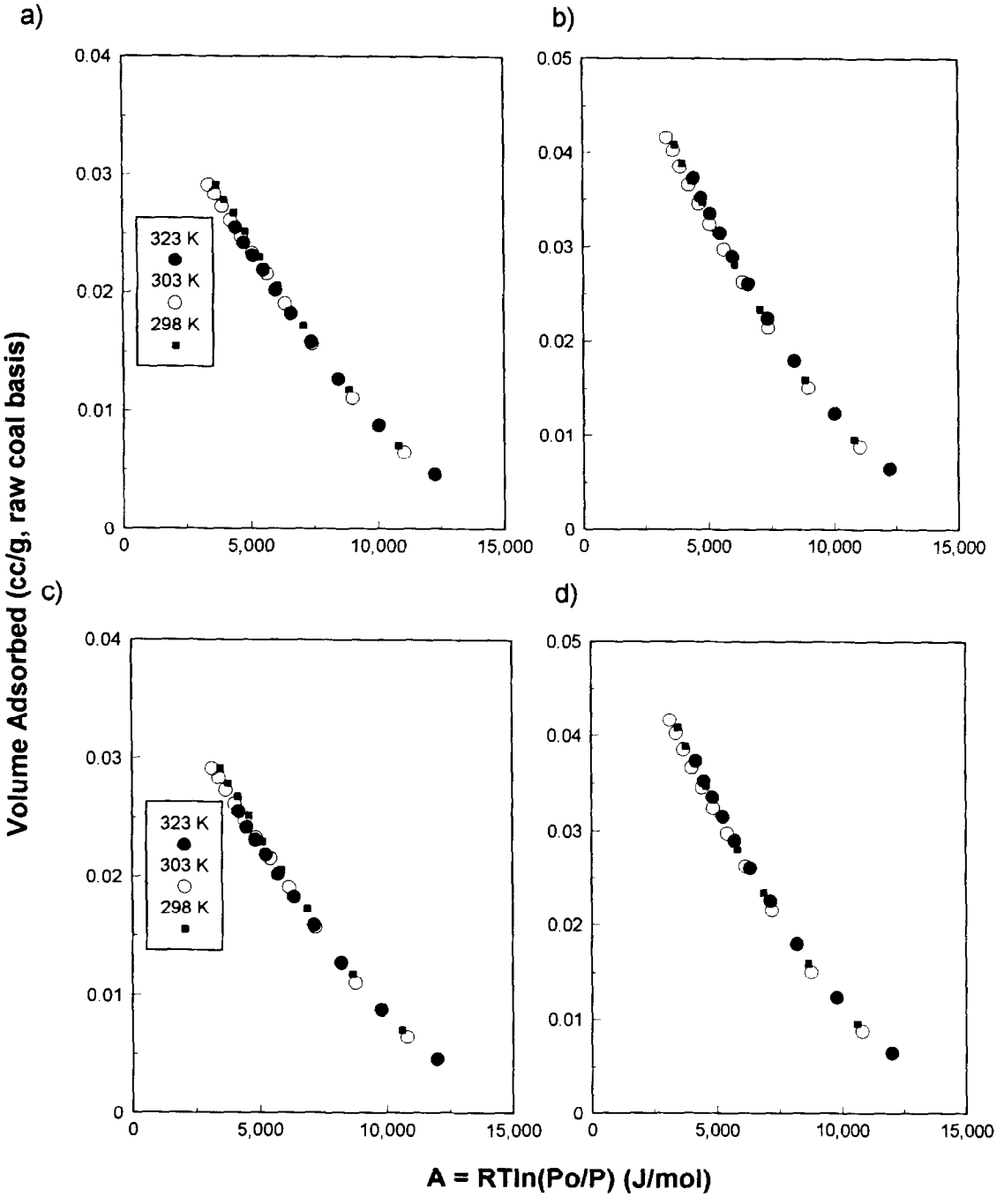

Fig. 8. Methane characteristic curves for sample GHA1-09. P_o was calculated using extrapolated vapour pressures (a,b) and the Kirchoff equation (c,d). Thermal expansion of the adsorbate is accounted for in (b) and (d).

(2) The monolayer volume, and hence the slope of the Langmuir plot, is temperature invariant.
(3) The fitting parameter B decreases exponentially with an increase in temperature.

Brunauer [33] showed that the Langmuir plot may not have a constant slope for the complete range of relative pressures, but may be subdivided into linear subsegments. This behaviour was attributed to surface heterogeneity. Several studies have shown that the monolayer amounts do vary with temperature, violating (2), but, as stated by Koresh [34], these experiments were performed at the same pressure range at different temperatures, and hence at higher temperatures, the isotherms represent less surface coverage. The consequent lower monolayer amounts may therefore be attributed to surface heterogeneity, as stated above. In this study, as with Koresh [34], criteria 1 and 2 will be considered as one.

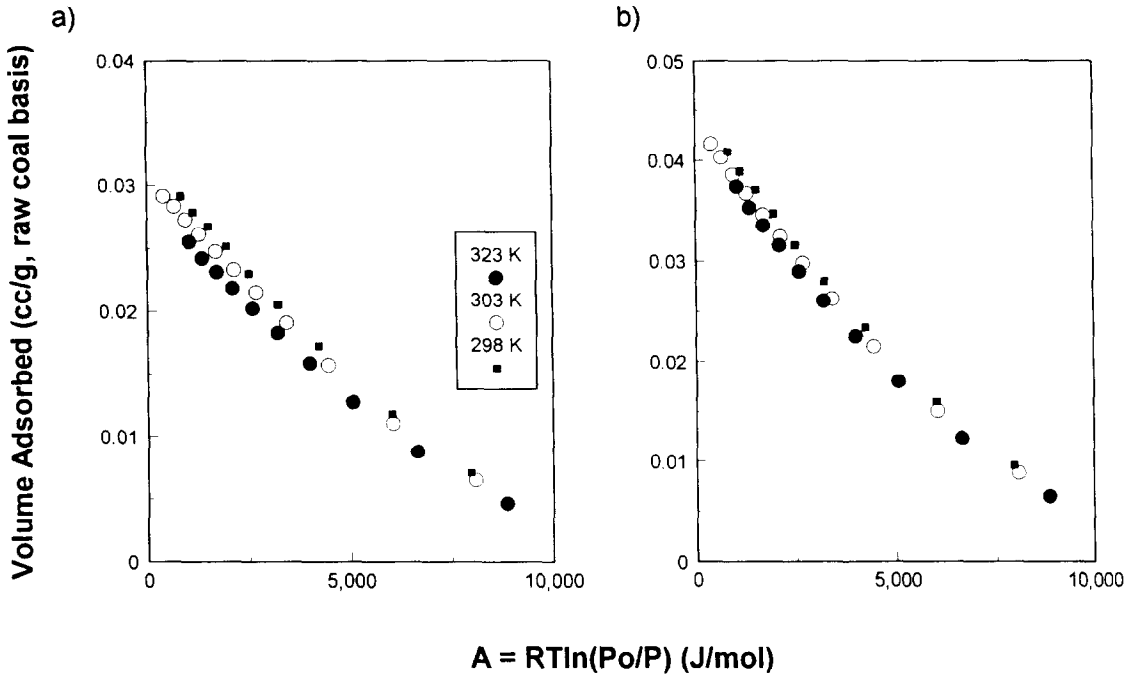

Fig. 9. Methane characteristic curves for sample GHA1-09. P_o was calculated using the Dubinin method. Thermal expansion of adsorbate is accounted for in (b).

Figure 6 shows the Langmuir plot (303 K isotherm data) for sample W1, along with a plot of the residuals. A line fit to the low pressure data (< 3 MPa) would yield a larger slope of the Langmuir plot compared to that at higher pressures, resulting in a smaller predicted monolayer volume at the lower pressures. In addition, the B constant would be larger. If the first three points of the Langmuir plot are used to calculate the monolayer volume, a value of 15.8 $cm^{-3}\,g^{-1}$ (DAF) is obtained, which is about 32% smaller than the value obtained from the entire range of pressure (23.1 $cm^{-3}\,g^{-1}$). Note that although sample W1 is an extreme case of the failure of the Langmuir model in this regard, all the samples studied show a similar trend to varying degrees.

Ruppel *et al.* [2] found that correcting for the change in dead space volume with gas adsorption actually introduced curvature into the Langmuir plot. In the current study, Langmuir plots were generated for uncorrected (no dead space correction) adsorbed volumes, and the curvature in the plots still existed (not shown). Correction for dead space error is therefore not the cause of curvature in the Langmuir plots shown.

According to 3, a plot of the parameter B versus temperature should be exponential in form [2] and this was demonstrated for sample GHA1-09 (not shown). Langmuir isotherms were recalculated by fitting a linear relationship between the (natural) logarithm of the experimentally-derived B parameter and the reciprocal temperature. These isotherms are shown in Fig. 7 along with the original experimentally determined isotherms. The fit to the original data is good with a relative error of around 2–3%. The Langmuir volumes determined from the Langmuir fit to each of the three isotherms separately were used in the recalculated Langmuir isotherms.

4.2 *Dubinin theory*

The thermal equation for adsorption may be written in the following form [22]:

$$\theta = F(A/E,n)$$

where θ is the degree of filling of the adsorption space; A is as defined previously (for vapours); E is the characteristic energy, which is equal to A at a particular value of θ; and n is a constant parameter. The function F is a distribution function of θ with respect to A; in the case of the D–A equation, the distribution adopted is that due to Weibull [35]. If E and n are temperature invariant parameters of this distribution, then the characteristic curve defined by the relationship $A = E\phi(\theta,n)$ should also be temperature invariant.

Methane adsorption characteristic curves for sample GHA1-09 at 298, 303 and 323 K were calculated to determine the effect of using several techniques for the determination of saturation pressure, adsorbed phase volume, differential molar work of adsorption (A), as well as for the correction for gas non-ideality. Table 3 outlines the various techniques utilized to obtain these parameters.

Figure 8 shows the characteristic plots for the case of no correction for gas non-ideality (pressure instead of fugacity), the assumption of liquid molar volume of the adsorbate at boiling point (Fig. 8(a)), and the

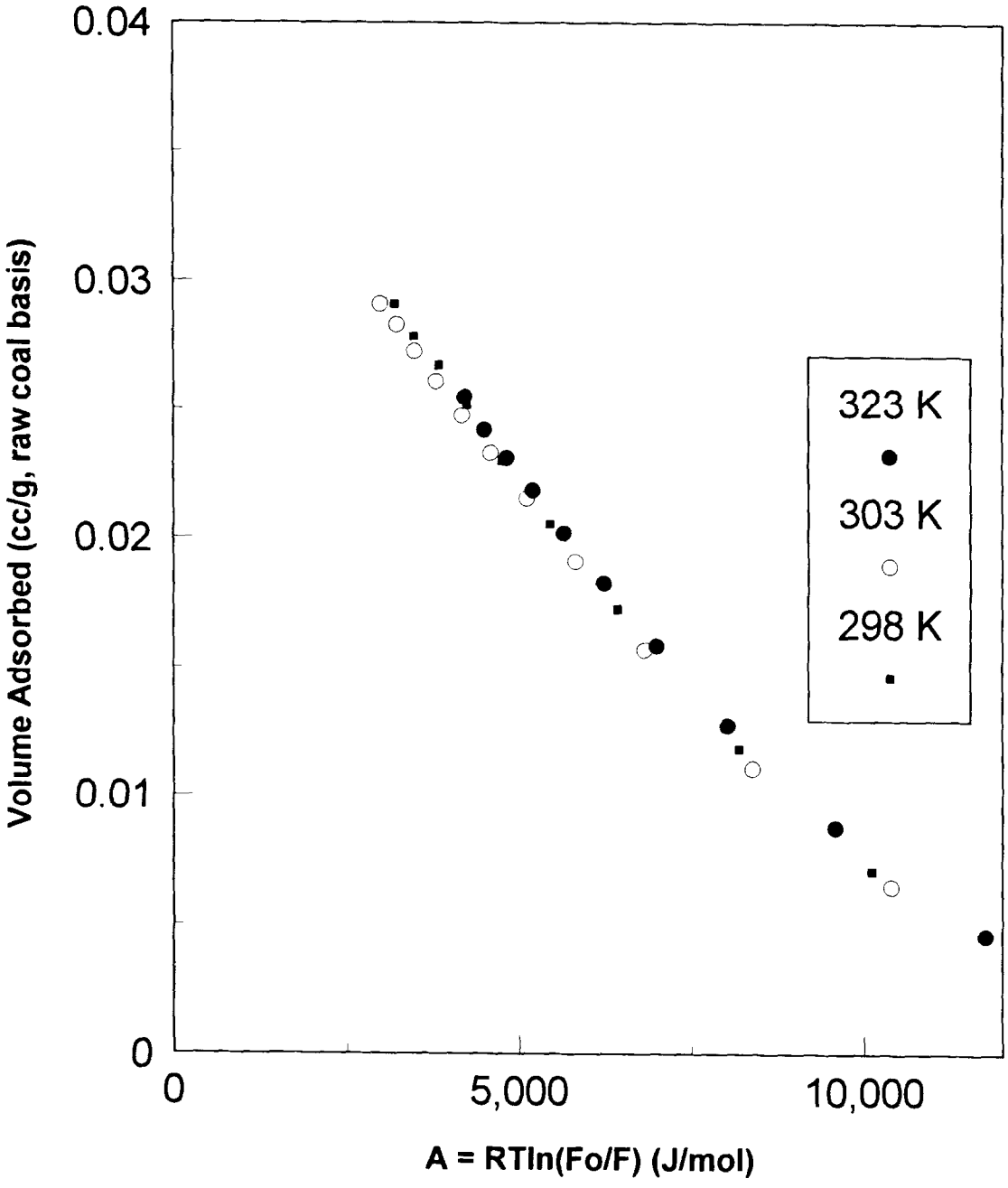

Fig. 10. Methane characteristic curves for sample GHA1-09 using fugacities instead of pressure.

calculated adsorbate molar volume using Dubinin's technique (Fig. 8(b)), which corrects for the thermal expansion of the adsorbate. For plots 8(a) and 8(b), the pseudo-saturation pressure was calculated using the extrapolation procedure discussed above. For the two plots, the maximum deviations from the characteristic curve are around $\pm 2\%$. Deviations are defined as the maximum deviation of adsorbed volume at a particular value of A divided by the maximum adsorption volume ($\times 100$) [11]. The correction for the thermal expansion of the adsorbate does not appear to have a significant effect upon the characteristic curve.

Characteristic curves calculated using the reduced Kirchoff equation to determine pseudo (extrapolated) vapour pressures are shown in Fig. 8(c) and (d). The maximum deviation for these plots is also about $\pm 2\%$. The use of the Kirchoff extrapolation for pseudo-vapour pressures in the calculation of the characteristic curves therefore yields similar results to those calculated using the extrapolation described above.

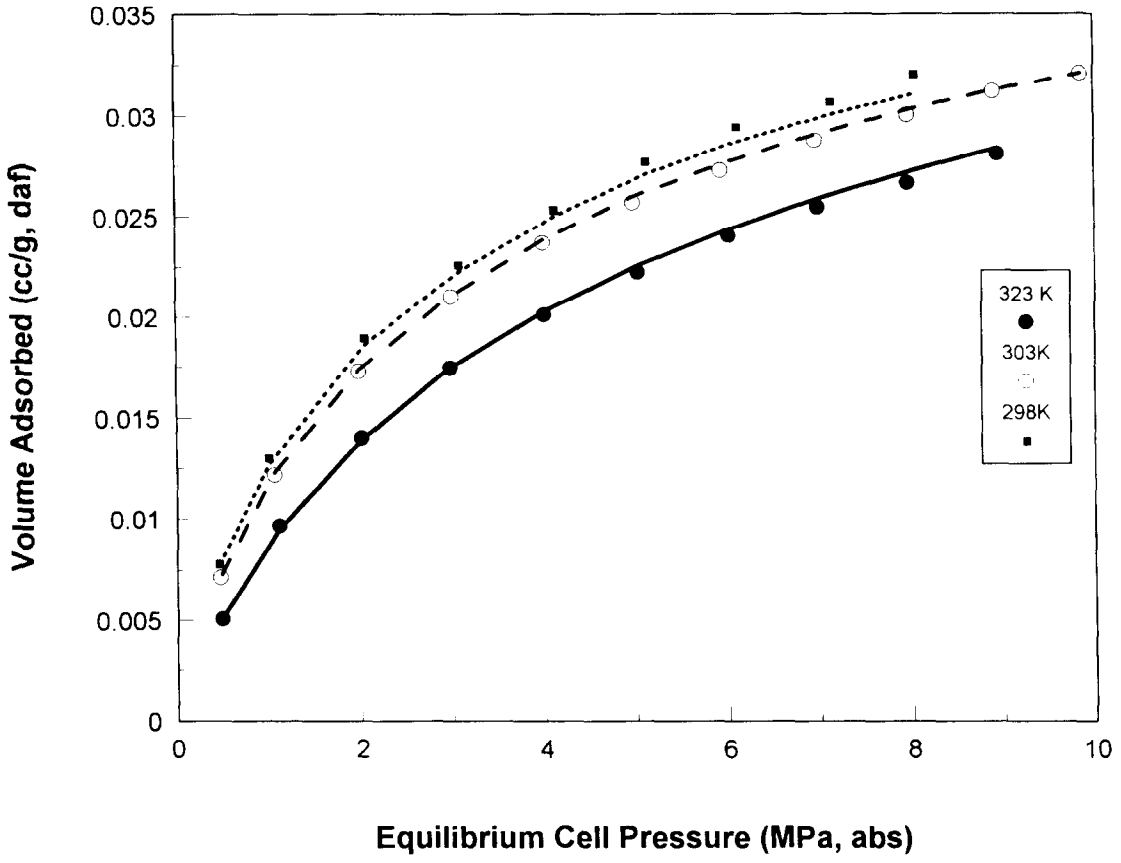

Fig. 11. Recalculated D A isotherms for GHA1-09.

Characteristic curves using the Dubinin technique for pseudo-vapour pressure extrapolation however display larger deviations than the other two vapour pressure extrapolation techniques (Fig. 9). The maximum deviation is over 4%. Correction for the thermal expansion of the adsorbate does appear to decrease the deviation from temperature invariance of the characteristic curve, however.

Correcting for non-ideality of the adsorbate vapour does not have a significant effect upon the characteristic curve. A characteristic curve calculated using the extrapolated vapour pressure technique and the assumption of a constant liquid density is shown in Fig. 10. Fugacities of the free-gas in equilibrium with the adsorbate are obtained by calculation of the fugacity coefficient using a virial series with Redlich–Kwong constants. This procedure is outlined in Noggle [36].

A plot of the experimental isotherms and the D–A fit calculated from the characteristic curve is shown in Fig. 11. The curve fit was performed by plotting log W vs A^n, where W is equal to the product of the number of moles of gas adsorbed and the liquid molar volume of methane at normal boiling point, A is the calculated differential molar work of adsorption and n is the optimized Astakhov coefficient (1.9). The curve fit appears to be reasonable, with an average relative error of less than 2%.

The characteristic curve for sample GHA1-09, plotted using the low pressure carbon dioxide data at 298 and 273 K and no correction for adsorbate density variation with temperature shows a deviation of up to 9%. Correction for adsorbate density, using the values of Toda *et al.* [35] at 273 and 298 K decreases the deviation to $\pm 2\%$ (Fig. 12). These results are in agreement with Toda *et al.* [37] who found that carbon dioxide adsorption at a variety of temperatures could be expressed by a single Dubinin–Polanyi plot.

There is some evidence that adsorption of carbon dioxide on coal may not be strictly physical adsorption. A study by Greaves *et al.* [38] demonstrated that high pressure sorption (up to about 7 MPa) of methane and carbon dioxide mixtures on dry coal exhibited hysteresis between the adsorption and desorption branches of the isotherm which became more pronounced with percentage of carbon dioxide used in the mix. The hysteresis was interpreted by the authors to be due to the retention of carbon dioxide preferentially over methane upon desorption. This experimental behaviour indicates that sorption of carbon dioxide in coal is not strictly due to

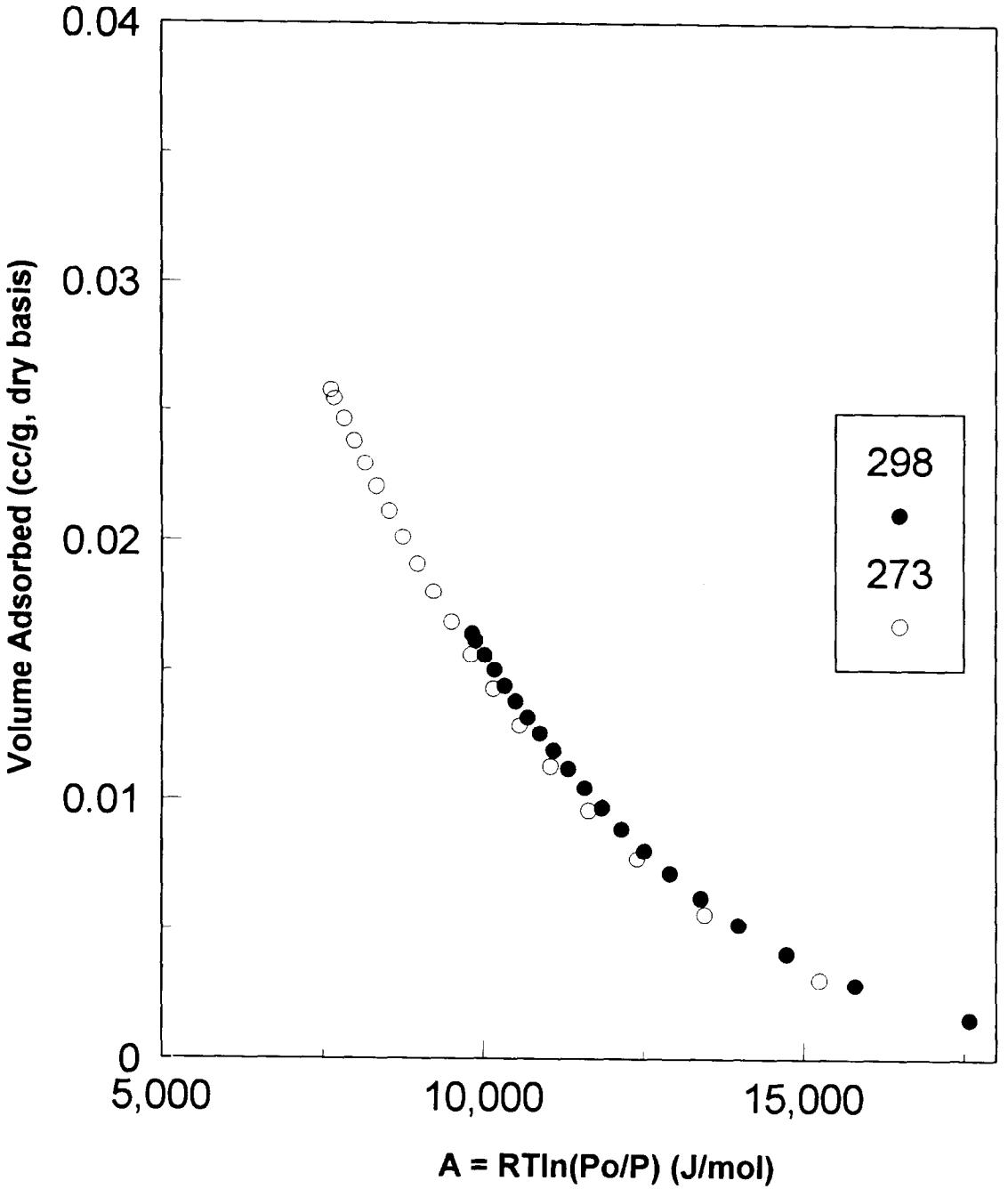

Fig. 12. Carbon dioxide characteristic curves for sample GHA1-09.

physical sorption. This phenomenon is currently being investigated.

In summary, high-pressure methane and low-pressure carbon dioxide adsorption characteristic curves are temperature-independent in the range of temperatures studied. The assumption of liquid density of the adsorbate for methane is sound and temperature dependence of this parameter need not be accounted for to attain temperature-invariant characteristic curves in the range of temperatures utilized here. For carbon dioxide, thermal expansion of the adsorbate must be accounted for, however. Of the several methods used to obtain pseudo-saturation pressures for methane, the extrapolation of the vapour pressure curve and the reduced Kirchoff equation are the best for calculating characteristic curves. The Dubinin technique for obtaining saturation pressures does not yield temperature-invariant characteristic curves regardless of the value used for adsorbate density. A recent study by Amankwah and Schwartz [12] has shown that a modified Dubinin equation for the attainment of pseudo-saturation fugacity yields better

results than the original Dubinin equation for high-pressure methane and hydrogen adsorption. The equation, however, introduces yet another parameter into the D–A equation that needs to be optimized.

5. CONCLUSIONS

A number of classical isotherm equations have been applied to model the adsorption of supercritical methane on coals at high pressures (up to 10 MPa) in an attempt to determine which yield the best curve-fit to the experimental data and which are the most physically realistic models. In addition carbon dioxide adsorption at low pressures on these same coals was analyzed by these equations.

The three-parameter Dubinin–Astakhov equation yields the best curve-fit to the high-pressure (>0.101 MPa) methane experimental data, but both the two-parameter Dubinin–Radushkevich and BET equations are better than the Langmuir equation. The same is true for the adsorption of carbon dioxide at low pressure (<0.127 MPa).

The validity of the monolayer and adsorption potential theories was also tested. The temperature dependence of the Langmuir B parameter is exponential in accordance with theory, although only three estimates of the parameter were obtained. The calculated isotherms from this relationship were in reasonable agreement with the experimental data. The assumption of an energetically homogeneous surface of adsorption is not strictly true, thus one of the postulates of Langmuir theory is violated for methane adsorption on coal.

In order to test the validity of potential theory, methane characteristic curves were plotted for a coal run at several temperatures. The curves are coincident if either the reduced Kirchoff equation or extrapolated vapour pressures are used to obtain the pseudo-saturation pressure of the adsorbate. The adsorbate is assumed to have the same density as the liquid adsorptive at the normal boiling point. Correction for thermal expansion of the adsorbate in the limited range of temperatures used here does not appear to be necessary, although the correction may be appropriate for a wider temperature range.

In the pressure and temperature range studied here, the adsorption potential theory for methane adsorption appears to be valid. For higher pressures, application of the BET isotherm equation may be more appropriate, but this requires further testing.

Low-pressure characteristic curves were also plotted for carbon dioxide at two different temperatures for the same coal. The characteristic curve for this adsorbate appears to be temperature-invariant only for the case where thermal expansion is corrected for.

Future studies will involve testing the validity of potential theory for high-pressure methane and carbon dioxide adsorption on a variety of coals at a wider range of temperatures than those applied here. In addition mixed gas analyses will be performed in order to test the validity of potential theory for these gases.

Acknowledgements—Funding for this study was provided by NSERC grant A-7337 to R. M. Bustin. The authors would like to thank Dr Cliff Stanley for his help with statistical analysis.

REFERENCES

1. Gregg, S. J. and Sing, K. S. W., *Adsorption, Surface Area and Porosity*, 2nd edn. Academic Press, New York, 1982.
2. Ruppel, T. C., Grein, C. T. and Beinstock, D., *Fuel*, 1974, **53**, 152.
3. Kim, A. G., U.S. Bureau of Mines Report of Investigations 8245, 1977.
4. Smith, D. M. and Williams, F. L., *SPEJ* (October), 1984, 529.
5. Hall, F. E., Zhou, C., Gasem, K. A. M. and Robinson Jr, R. L., *SPE* 29194, paper presented at the 1994 Eastern Regional Conference and Exhibition, Charleston, WV, November 8–10, 1994, p. 329.
6. Polanyi, M., *Science*, 1963, **141**, 1010.
7. Lewis, W. K., Gilliland, E. R., Chertow, B. and Cadogen, W. P., *Ind. Eng. Chem.*, 1950, **42**, 1319.
8. Maslan, F. D., Altman, M. and Alberth, E. R., *J. Phys. Chem.*, 1953, **57**, 106.
9. Grant, R. J., Manes, M. and Smith, S. B., *AIChEJ.*, 1964, **8**, 403.
10. Cook, W. H. and Basmadjian, D., *Can. J. Chem. Eng.*, 1964, **42**, 146.
11. Agarwal, R. K. and Schwartz, J. A., *Carbon*, 1988, **26**, 873.
12. Amankwah, K. A. G. and Schwartz, J. A., *Carbon*, 1995, **33**, 1313.
13. Yang, J. T., *Gas Separation by Adsorption Processes*. Butterworth Publishers, London, 1987.
14. Yang, R. T. and Saunders, J. T., *Fuel*, 1985, **64**, 616.
15. Mavor, M. J., Owen, L. B. and Pratt, T. J., *SPE* 20728, paper presented at the SPE 65th Annual Technical Conference and Exhibition, New Orleans, LA, September 23–26, 1990b, p. 157.
16. Harpalani, S. and Pariti, U. M., in *Proceedings of the 1993 International Coalbed Methane Symposium*. The University of Alabama/Tuscaloosa, May 17–21, 1993, p. 151.
17. Langmuir, I., *J. Am. Chem. Soc.*, 1918, **40**, 1361.
18. Bell, G. J. and Rakop, K. C., *SPE* 15454, paper presented at the SPE 61st Annual Technical Conference and Exhibition, New Orleans, LA, October 5–8, 1986, p. 1.
19. Brunauer, S., Emmett, P. H. and Teller, E., *J. Am. Chem. Soc.*, 1938, **60**, 309.
20. Lowell, S. and Shield, J. E., *Powder Surface Area and Porosity*, 2nd edn. Chapman and Hall, London, 1984.
21. Dubinin, M. M., in *Chemistry and Physics of Carbon*, Vol. 2, ed. P. L. Walker, Jr. Edward Arnold, Ltd., New York, 1966.
22. Dubinin, M. M., in *Progress in Surface and Membrane Science*, Vol. 9, Ch. 1, ed. D. A. Cadenhead *et al.* Academic Press, New York, 1975.
23. Kapoor, A., Ritter, J. A. and Yang, R. T., *Langmuir*, 1989, **5**, 1118.
24. Bering, B. P., Dubinin, M. M. and Serpinsky, V. V., *J. Colloid Int. Sci.*, 1966, **21**, 378.
25. Wakasugi, Y., Ozawa, S. and Ogino, Y., *J. Colloid Int. Sci.*, 1976, **79**, 399.
26. Ozawa, S., Kusumi, S. and Ogino, Y., *J. Colloid Int. Sci.*, 1981, **56**, 83.
27. Bustin, R. M., Clarkson, C. R. and Levy, J., paper presented at the Twenty Ninth Newcastle Symposium

on "Advances in the Study of the Sydney Basin". Newcastle, NSW, Australia, April 6–9, 1995.
28. Bustin, R. M., Cameron, A. R., Grieve, D. A. and Kalkreuth, W. D., *Coal Petrology: Its Principles, Methods and Applications*, 2nd edn. Geological Association of Canada Short Course Notes 3, 1985.
29. Levy, J. H., Killingley, J. S., Day, S. J. and Liepa, I., in *Proceedings of the Symposium on Coalbed Methane Research and Development in Australia.* Townsville, Queensland, Australia, 1992.
30. *Handbook of Chemistry and Physics*, section **6**-82, 71st edn., editor-in-chief David R. Lide. CRC Press, Boston, USA 1990–1991.
31. Yee, D., Seidle, J. P. and Hanson, W. B., in *Hydrocarbons from Coal*, AAPG Studies in Geology #38, Ch. 9, ed. B. E. Law and D. D. Rice. The American Association of Petroleum Geologists, Tulsa, Oklahoma, USA 1993, p. 203.
32. Marsh, H. and Siemieniewska, T., *Fuel*, 1965, **44,** 355.
33. Brunauer, S., *The Adsorption of Gases and Vapors*, Vol. 1. Princeton University Press, Princeton, 1943.
34. Koresh, J., *J. Colloid Int. Sci.*, 1982, **88,** 398.
35. Dubinin, M. M. and Astakhov, V. A., in *Advances in Chemistry Series*, No. 102. American Chemical Society Publications, Washington D.C. 1971, p. 102.
36. Noggle, J. H., *Physical Chemistry*, 2nd edn. Harper Collins Publishers, New York, NY 1989.
37. Toda, Y., Hatami, M., Toyoda, S., Yoshida, Y. and Honda, H., *Fuel*, 1971, **50,** 187.
38. Greaves, K. H., Owen, L. B. and McLennan, J. D., in *Proceedings of the 1993 International Coalbed Methane Symposium.* The University of Alabama/Tuscaloosa, May 17–21, 1993, p. 151.